Effect of the Two Conserved Prolines of Human Growth Inhibitory Factor (Metallothionein-3) on Its Biological Activity and Structure Fluctuation: Comparison with a Mutant Protein†

Daniel W. Hasler,‡ Laran T. Jensen,§ Oliver Zerbe,|| Dennis R. Winge,§ and Milan Vašák*,‡

Institute of Biochemistry, University of Zürich, and Department of Pharmacy, ETH, Winterthurerstrasse 190, CH-8057 Zürich, Switzerland, and Department of Biochemistry, University of Utah Health Science Center, Salt Lake City, Utah 84132

Received July 6, 2000; Revised Manuscript Received September 18, 2000

ABSTRACT: Human neuronal growth inhibitory factor, a metalloprotein classified as metallothionein-3 (MT-3), impairs the survival and the neurite formation of cultured neurons. In these studies the double P7S/P9A mutant (mutMT-3) and single mutants P7S and P9A of human Zn_7-MT-3 were generated, and their effects on the biological activity and the structure of the protein were examined. The biological results clearly established the necessity of both proline residues for the inhibitory activity, as even single mutants were found to be inactive. Using electronic absorption, circular dichroism (CD), magnetic CD (MCD), and ^{113}Cd NMR spectroscopy, the structural features of the metal−thiolate clusters in the double mutant Cd_7-mutMT-3 were investigated and compared with those of wild-type Cd_7-MT-3 [Faller, P., Hasler, D. W., Zerbe, O., Klauser, S., Winge, D. R., and Vašák, M. (1999) *Biochemistry 38*, 10158] and the well characterized Cd_7-MT-2a from rabbit liver. Similarly to $^{113}Cd_7$-MT-3 the ^{113}Cd NMR spectrum of $^{113}Cd_7$-mutMT-3 at 298 K revealed four major and three minor resonances (approximately 20% of the major ones) between 590 and 680 ppm, originating from a Cd_4S_{11} cluster in the α-domain and a Cd_3S_9 cluster in the *β*-domain, respectively. Due to the presence of dynamic processes in the structure of MT-3 and mutMT-3, all resonances showed the absence of resolved homonuclear [$^{113}Cd-^{113}Cd$] couplings and large apparent line widths (between 140 and 350 Hz). However, whereas in $^{113}Cd_7$-mutMT-3 the temperature rise to 323 K resulted in a major recovery of the originally NMR nondetectable population of the Cd_3S_9 cluster resonances, no such temperature effect was observed in $^{113}Cd_7$-MT-3. To account for the observed NMR features, a dynamic structural model for the *β*-domain is proposed, which involves a folded and a partially unfolded state. It is suggested that in the partially unfolded state a slow *cis/trans* isomerization of Cys-Pro(7) or Cys-Pro(9) amide bonds in $^{113}Cd_7$-MT-3 takes place and that this process represents a rate-limiting step in a correct domain refolding. In addition, closely similar apparent stability constants of human MT-3, mutMT-3, and rabbit MT-2a with Cd(II) and Zn(II) ions were found. These results suggest that specific structural features dictated by the repetitive $(Cys\text{-}Pro)_2$ sequence in the *β*-domain of MT-3 and not its altered metal binding affinity compared to MT-1/MT-2 isoforms are responsible for the biological activity of this protein.

The pathological pattern of Alzheimer's disease (AD)[1] is characterized by the progressive loss of neurons accompanied by the formation of intraneural neurofibrillary tangles and extracellular amyloid plaques (*1*). One hypothesis postulated that these alterations are caused by an imbalance of neurotrophic factors (*2*). Performing in vitro cell culture studies, Uchida et al. (1988) discovered that protein extract from AD brain increased rat cortical neuron survival more effectively than extract from normal human brain, suggesting that AD brain possesses elevated neurotrophic activity (*3*). This apparent increase in neurotrophic activity in AD brain was found to be due to the loss of a growth inhibitory factor which was subsequently purified from healthy human brains (*4*). Its characterization revealed a metalloprotein of 68 amino acids containing 4 copper and 3 zinc ions with its primary structure exhibiting approximately 70% sequence identity with those of mammalian metallothioneins (MT-1/MT-2 isoforms: 61 or 62 amino acids), including the preserved array of 20 cysteine residues (*4*). These features together with molecular biological studies led to its classification as

† This work was supported in part by Swiss National Science Foundation Grant 31-58858.99, Stipendienfonds der Basler Chemischen Industrie (D.W.H.), and NIH Grant 03817 to D.R.W.

* To whom correspondence should be addressed. Tel: (+41)-1-635 5552. Fax: (+41)-1-635 6805.

‡ University of Zürich.

§ University of Utah Health Science Center.

|| ETH.

[1] Abbreviations: AD, Alzheimer's disease; MT, metallothionein; MT-3, metallothionein-3 isoform; mutMT-3, double mutant P7S/9PA of MT-3; CD, circular dichroism; MCD, magnetic circular dichroism; ESI-MS, electrospray ionization mass spectrometry; EXAFS, extended X-ray absorption fine structure; LMCT, ligand-to-metal charge transfer; BAPTA, 1,2-bis(2-aminophenoxy)ethane-*N*,*N*,*N*′,*N*′-tetraacetic acid; 5F-BAPTA, 1,2-bis(2-amino-5-fluorophenoxy)ethane-*N*,*N*,*N*′,*N*′-tetraacetic acid; PBS, phosphate-buffered saline.

10.1021/bi001569f CCC: $19.00
Published on Web 11/02/2000

MT-3 (*5*, *6*). Compared to the amino acid sequences of mammalian MT-1/MT-2, the consensus sequence of MT-3 contains two inserts: a single Thr in the N-terminal region and a Glu-rich hexapeptide in the C-terminal region. Additionally, all known MT-3 sequences contain the conserved C(6)-P-C-P(9) motif, which is absent in all other members of the MT family (*4*, *5*, *7*−*10*).

Despite the high similarities between the primary structures of MT-3 and mammalian MT-1/MT-2, the biological properties of these two proteins differ. In neuronal cell culture studies only MT-3 but not MT-1/MT-2 exhibits a growth inhibitory activity (*4*, *11*, *12*). A comparative study investigated the growth inhibitory activity of recombinant Zn_7-MT-3 and its individual protein domains reconstituted with Zn(II) ions, i.e., the N-terminal β-domain (residues 1−32) and the C-terminal α-domain (residues 32−68). In these studies Zn_7-MT-3 and the Zn_3-β-domain were found to possess the same level of growth inhibitory activity, whereas the Zn_4-α-domain was found to be inactive (*13*). Most interestingly, the growth inhibitory activity of the isolated Zn_3-β-domain was abolished by mutating the two proline residues in MT-3 either to the C(6)-S-C-A(9) sequence found in human MT-2 or to the C(6)-T-C-T(9) sequence (*13*). The observed differences in biological activity point to particularities of the MT-3 structure caused by the presence of these proline residues. Proline residues are often found at important positions in proteins and greatly affect the protein secondary structure (*14*). Recently, it has been demonstrated that the spectroscopic properties of a $M^{II}{}_3S_9$ cluster formed with Zn(II) and Cd(II) ions in the individual β-domain of human MT-3 widely differ from those found for a cyclohexane-like $M^{II}{}_3S_9$ cluster in the corresponding part of mammalian $M^{II}{}_7$-MT-2, suggesting that substantial differences between these structures exist (*15*).

The present work was conducted with the aim of gaining insights into the effect of the conserved C(6)-P-C-P(9) motif on the entire protein structure and its biological activity. For this purpose, double and single human MT-3 mutants were generated in which the proline residues were replaced by the corresponding amino acid residues of human MT-2. The inhibitory activity of the zinc-containing double mutant P7S/P9A of MT-3 (mutMT-3) and the single mutants P7S and P9A was tested in neuronal cell cultures and compared with that of Zn_7-MT-3. The structural features of the biologically inactive double mutant mutMT-3 were further investigated by electronic absorption, circular dichroism (CD), magnetic CD (MCD), and ^{113}Cd NMR spectroscopy. The results obtained on Cd_7-mutMT-3 were compared with those of human Cd_7-MT-3 (*16*) and the structurally well-characterized Cd_7-MT-2a from rabbit liver (*17*). In addition, the apparent metal-binding constants of MT-3, mutMT-3, and rabbit MT-2a with Cd(II) and Zn(II) ions were determined. In the determination of the Cd(II)-binding constants a spectrophotometric pH titration method was applied. For the Zn(II)-binding constants a ^{19}F NMR based method, previously developed for the measurement of free intracellular metal concentrations, was adapted. In this case a competition between the Zn(II)-containing protein and the complexing agent 5F-BAPTA was monitored by ^{19}F NMR. The structural properties of wild-type MT-3 likely to be responsible for its biological function are discussed.

MATERIALS AND METHODS

Expression and Purification of MT-3. Human MT-3, mutMT-3, and the single mutants P7S-MT-3 and P9A-MT-3 were cloned, expressed, and purified as described (*13*, *16*). The molecular masses of the apoproteins were determined by ESI-MS (SCIEX API III$^+$) revealing masses of 6926 and 6890 Da for MT-3 and mutMT-3, respectively, which correspond well to the calculated masses of 6927 and 6891 Da. Rabbit MT-2a was isolated from rabbit livers as reported (*18*).

The Zn_7 and Cd_7 forms of MT-3, mutMT-3, and MT-2a were generated by the method of Vašák (*19*). Metal-to-protein ratios were determined by measuring the metal concentration by atomic absorption spectrometry (IL Video 12 or Perkin-Elmer 305) and the protein concentration via sulfhydryl concentration (20 Cys per protein). In the latter case the sulfhydryl reaction with 2,2′-dithiopyridine in 0.2 M sodium acetate and 1 mM EDTA (pH 4) was followed spectroscopically and the concentration determined using $\epsilon_{343} = 7600\ M^{-1}\ cm^{-1}$ (*20*). For all proteins, i.e., MT-3, mutMT-3, P7S-MT-3, P9A-MT-3, and MT-2a, a metal-to-protein ratio of 7 ± 0.15 was obtained.

Spectroscopic Measurements. Absorption spectra were recorded on a Cary 3 spectrometer. CD and MCD measurements were made using a Jasco (Model J-715) spectropolarimeter equipped with a 1.5 T electromagnet for room temperature MCD measurements. The CD spectra are expressed as molar ellipticity, [Θ], in units of deg dmol^{-1} cm^2, and the MCD spectra are expressed as [Θ_M] in units of deg dmol^{-1} cm^2 T^{-1}. The ^{113}Cd NMR spectra were recorded on a Bruker AMX-600 spectrometer using an inverse gated broad-band proton decoupling, a 62500 Hz spectral width, a 0.13 s aquisition time, and a 0.4 s pulse repetition rate. Signal saturation could be ruled out as ^{113}Cd NMR spectra obtained with a 2 s repetition rate did not show any intensity enhancement of the resonances. ^{19}F NMR spectra were recorded on the same NMR spectrometer with a 10 000 Hz spectral width, a 0.27 s acquisition time, and a 2 s pulse repetition rate. All NMR samples contained 10% ^2H_2O to provide the field-frequency lock and were measured in 5 mm NMR tubes. The ^{113}Cd resonances are given in parts per million relative to the external standard 0.1 M $Cd(ClO_4)_2$ and those of ^{19}F relative to the external standard $CFCl_3$.

Neuron Survival Assay. Neonatal rat cortical cell cultures were prepared and maintained as previously described (*11*). The cells were plated into serum-free MEM N2 medium. Approximately 1 h later the cultures were supplemented with one of the following: Alzheimer's disease brain extract (240 μg of protein mL^{-1}), purified Zn_7-MT-3 dissolved in sterile phosphate-buffered saline (PBS), or both AD brain extract and MT-3. AD brain extract was freshly prepared as previously described (*11*) from the frontal cortex of brain fulfilling all criteria for the diagnosis of AD. The quantity of Zn_7-MT-3 added was restricted to <20 μg/mL to avoid precipitation in the mixture. The number of surviving neurons was quantified after 3 days by microscopic examination of four random fields, using immunocytochemical staining with anti-MAP2 primary antibodies (*11*). The biological activity of Zn_7-mutMT-3, Zn_7-P7S-MT-3, Zn_7-P9A-MT-3, and mouse Zn_7-MT-1 was examined in the same manner.

Table 1: Amino Acid Sequences of Human MT-3 and Mammalian MT-1 and MT-2

β-domain			
human MT-3	1	MDPETCPCPS·GGSCTCADSCKCEGCKCTSCK	31
mutMT-3	1	MDPETCSCAS·GGSCTCADSCKCEGCKCTSCK	31
rabbit MT-2a	1	MDPN·CSCAAAGDSCTCANSCTCKACKCTSCK	31
mouse MT-1	1	MDPN·CSCST·GGSCTCTSSCACKNCKCTSCK	30
α-domain			
human MT-3	32	KSCCSCCPAECEKCAKDCVCKGGEAAEAEAEKCSCCQ	68
mutMT-3	32	KSCCSCCPAECEKCAKDCVCKGGEAAEAEAEKCSCCQ	68
rabbit MT-2a	32	KSCCSCCPPGCAKCAQGCICKG·····ASDKCSCCA	62
mouse MT-1	31	KSCCSCCPVGCSKCAQGCVCKG·····AADKCTCCA	61

Determination of Cd(II)-Binding Constants by Photometric pH Titration. The apparent Cd(II)-binding constants of Cd_7-MT-2a, Cd_7-MT-3, and Cd_7-mutMT-3 at pH 7.0 were calculated as previously described by Kägi et al. (*21*, *22*) using the adapted expression of Wang et al. (*23*). In brief, the release of Cd(II) bound to the proteins was achieved by stepwise lowering of the pH with HCl. A stock solution of either Cd_7-MT-2a, Cd_7-MT-3, or Cd_7-mutMT-3 in 10 mM Tris and 20 mM NaCl, pH 8.0, was diluted about 20 times with N_2-saturated water. Two milliliters of the diluted sample (approximately 6 μM) was placed in a 1 cm cuvette. The starting protein concentration was determined by measuring the Cd content by atomic absorption spectrometry, assuming a metal-to-protein ratio of 7. Prior to the titration the samples were purged with N_2 for several minutes. The pH was measured directly in the cuvette with a pH microelectrode (MI-414, Microelectrodes Inc., Bedford). The pH was lowered by addition of small aliquots of 0.1 M HCl, and the metal release was followed by recording an absorption spectrum at approximately each 0.05 pH step. The volume changes due to the addition of HCl were neglected (less than 1.5%). The degree of Cd(II) release from the proteins is illustrated by plotting the pH values against the percentage of metal dissociation described by

$$D = \frac{A_{250i} - A_{250,\mathrm{pH}=1}}{A_{250,\mathrm{pH}=8} - A_{250,\mathrm{pH}=1}}$$

where A_{250i} is the absorption of the Cd(II)−thiolate complex at 250 nm at the various pH values and $A_{250,\mathrm{pH}=8}$ and $A_{250,\mathrm{pH}=1}$ represent the corresponding absorption of the Cd_7 and the apoprotein, respectively. However, since in contrast to Cd_7-MT-2a the pH titration profiles of both Cd_7-MT-3 and Cd_7-mutMT-3 did not display a pronounced two-step titration profile, for these MT-3 forms only the overall apparent binding constants were calculated using an average number of thiolate ligands bound to Cd(II) ($n = 2.85$), which reflects the CysS-to-Cd(II) stoichiometry in the three proteins. In all cases, the pK_a values of the cysteine side chains were assumed to be equal to those of rabbit MT isoforms (pK_a = 8.9) (*21*).

Determination of Zn-Binding Constants by 5F-BAPTA ^{19}F NMR. The ^{19}F NMR spectra of a mixture of 5F-BAPTA and either Zn_7-MT-2a, Zn_7-MT-3, or Zn_7-mutMT-3 were measured. 5F-BAPTA was obtained from Molecular Probes Inc. (Eugene, OR). The pH of a 100 mM stock solution of 5F-BAPTA in 10 mM Tris was adjusted to pH 8.0 with HCl/NaOH. The NMR samples typically contained 2 mM 5F-BAPTA and 65 μM Zn_7-MT-2a, Zn_7-MT-3, or Zn_7-mutMT-3 in 10 mM Tris-HCl, pH 8.0, and 10% D_2O. This protein concentration corresponds to a Zn-binding site concentration of 455 μM, the binding sites being considered to be independent and equal. To ensure that thermodynamic equilibrium was reached, the samples were allowed to equilibrate for 3 h at room temperature before the ^{19}F NMR spectra were acquired. Note that in rabbit Cd_7-MT-2a the half-life for metal exchange ranges between 0.5 s and 16 min for the β- and α-domains, respectively (*24*). The well-separated ^{19}F signals of free 5F-BAPTA and Zn-5F-BAPTA were integrated using the Bruker WIN NMR software package. The apparent binding constant of Zn-5F-BAPTA was corrected for the conditions applied in this measurement (pH, salt concentration, buffer, temperature) as described (*25*), using the program Chelator (*26*). In the calculation, the initial binding constant K for the Zn-5F-BAPTA complex of 1.3×10^8 M^{-1} (30 °C, 40 mM HEPES, pH 7.1, ionic strength 0.138 M) (*25*) was used and recalculated for the conditions of the NMR measurements (25 °C, 10 mM Tris-HCl, pH 8.0, ionic strength 4 mM). The resulting value was $K = 4.3 \times 10^9$ M^{-1}. This stability constant was used to determine the apparent binding constants for Zn_7-MT-2a, Zn_7-MT-3, and Zn_7-mutMT-3, applying the expression derived in the Appendix (see paragraph at end of paper regarding Supporting Information).

RESULTS

Bioactivity of MT-3, Mutant Variants, and Mouse MT-1. All biological cell culture studies were carried out with the Zn(II)-containing forms as Cd(II) ions are neurotoxic. Previously, it has been shown that the synthetic β-domain peptide (residues 1−31) of human MT-3 containing three Zn(II) ions exhibits growth inhibitory activity and that a mutation of the proline residues in the unique C(6)-P-C-P(9) motif to the amino acids commonly found in mammalian MT-1/MT-2 abolishes the inhibitory activity (*13*). To verify that the proline residues in MT-3 at positions 7 and 9 are indeed critical for the growth inhibitory activity, these residues were mutated in the full-length human Zn_7-MT-3 (Table 1). For comparison, the biologically inactive mouse Zn_7-MT-1 was also included in the activity assay. The relative survival of the cultured neurons as a function of increasing concentrations of added protein is depicted in Figure 1. Thus, while wild-type Zn_7-MT-3 inhibited the cell growth in a concentration-dependent manner, no inhibitory effect was found with the double mutant P7S/P9A-MT-3 (mutMT-3). At higher concentrations of the wild-type protein

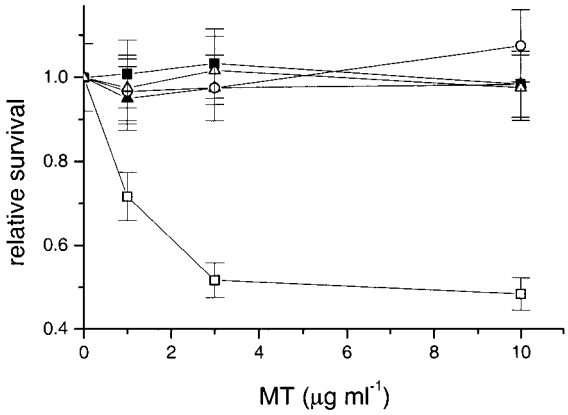

FIGURE 1: Effect of proline substitution in MT-3 on the survival of cortical neurons. Human Zn_7-MT-3 (□), human Zn_7-mutMT-3 (○), Zn_7-P7S-MT-3 (■), Zn_7-P9A-MT-3 (△), and mouse Zn_7-MT-1 (▲) were tested for their ability to inhibit the survival of cortical neurons supplemented with AD brain extract. Double mutations at proline residues 7 and 9 resulted in the loss of the growth inhibitory activity as did mutation of each single proline residue individually. The inactive mouse Zn_7-MT-1 is included for comparison.

the growth inhibition reaches a plateau at about 50% of relative neuron survival. In the previous neuronal cell culture studies, a similar level of inhibitory activity for Zn_7-MT-3 has also been found (*11*). In these studies, both control and AD brain extracts showed a stimulating effect on neuronal survival. However, AD extracts enhanced the survival of neurons approximately 2-fold relative to control extract at all doses tested. Thus, MT-3 negates the increased neuronal survival caused by AD extracts. To test whether one or both of the proline residues are critical for the activity, single mutants were also generated, and their activity was assessed. Both single mutants, Zn_7-P7S-MT-3 and Zn_7-P9A-MT-3, did not show any growth inhibitory activity, indicating that the presence of both proline residues is essential for the biological activity of MT-3 (Figure 1).

Electronic Absorption, CD, and MCD Studies. To examine the underlying structural changes leading to the loss of biological activity, the spectroscopic characterization of the Cd(II) derivative of mutMT-3 was conducted. The spectroscopic properties of Cd_7-mutMT-3 were compared with those of Cd_7-MT-3 characterized in our previous studies (*16*). Since the three-dimensional structure of MT-3 is not known and since the two proline residues are missing in the mammalian MT family, the spectroscopic features were compared with those of the structurally well-characterized Cd_7-MT-2a from rabbit liver (*17*). It may be noted that due to the absence of aromatic amino acids in mammalian MTs, the spectral features above 230 nm are dominated by metal-induced transitions.

The electronic absorption, CD, and MCD spectra of Cd_7-mutMT-3, Cd_7-MT-3, and Cd_7-MT-2a are presented in Figure 2. The electronic absorption and MCD spectra of all three proteins are closely similar. The former are characterized by a metal-induced shoulder at about 250 nm due to CysS−Cd(II) LMCT transitions (*27*, *28*). The molar extinction coefficient at 250 nm for all three proteins ($\epsilon_{250} \approx 1 \times 10^5$ M^{-1} cm^{-1}) reveals a value of 5×10^3 M^{-1} cm^{-1} per cysteine ligand (20 Cys are present). This value is similar to that found for the lowest energy CysS−Cd(II) LMCT transition at about 250 nm in a number of Cd-substituted metalloproteins (*29*),

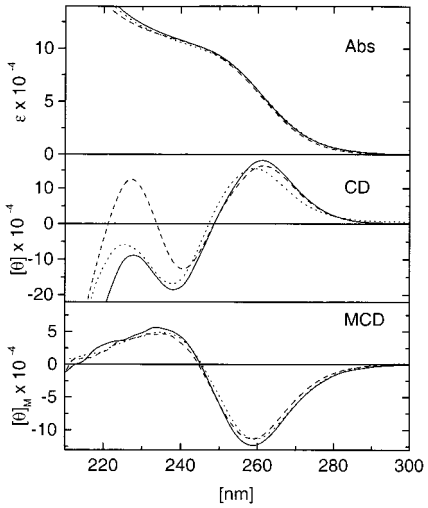

FIGURE 2: Electronic absorption (Abs), circular dichroism (CD), and magnetic circular dichroism (MCD) spectra of human Cd_7-mutMT-3 (—), human Cd_7-MT-3 (- - -), and rabbit liver Cd_7-MT-2 (— —) in 25 mM Tris-HCl and 50 mM NaCl, pH 8.0.

indicating that all 20 Cys−thiolates are involved in metal coordination. The MCD spectra of the three proteins show a similar profile with bands at (−)260 and (+)238 nm. In rat Cd_7-MT this biphasic profile has been assigned to a positive *A* term, originating from Cd(II) sites possessing a T_d type of symmetry (*30*). In contrast, the corresponding CD spectra, which are highly sensitive to structural changes, exhibit pronounced differences in shape, intensity, and position of the CD bands. Whereas the CD spectrum of rabbit Cd_7-MT-2a shows extrema at (+)261, (−)241, and (+)228 nm, the extrema of Cd_7-MT-3 are found at (+)259, (−)238, and (+)225 nm and those of mutMT-3 at (+)261, (−)238, and (+)228 nm (Figure 2). The low-energy CysS−Cd(II) LMCT transition in all three Cd_7 proteins is characterized by a biphasic CD profile with a crossover point around 250 nm. In Cd_7-MT from various species this feature has been assigned to an excitonic coupling between transition dipole moments of the bridging thiolate ligands within the cluster structure (*31*).

^{113}Cd NMR Studies. The ^{113}Cd isotope is often used to probe Zn(II) sites in proteins by ^{113}Cd NMR spectroscopy. The ^{113}Cd NMR spectrum of $^{113}Cd_7$-mutMT-3 recorded at 298 K is depicted in Figure 3 C. The spectrum reveals four major resonances at 676, 624, 622, and 595 ppm and three minor resonances at about 670, 650, and 635 ppm. All resonances are lacking resolved homonuclear [^{113}Cd−^{113}Cd] couplings and show a large apparent line width (between 150 and 350 Hz). Similar features have also been observed in the corresponding ^{113}Cd NMR spectrum of $^{113}Cd_7$-MT-3 (Figure 3A) (*16*). Upon heating the samples to 323 K all lines of $^{113}Cd_7$-MT-3 and $^{113}Cd_7$-mutMT-3 became sharper (Figure 3B,D), due mainly to decreased correlation time. In the case of $^{113}Cd_7$-mutMT-3 the intensity of three minor ^{113}Cd resonances increased (see below). However, even under these conditions the signals were still very broad, and the homonuclear [^{113}Cd−^{113}Cd] couplings remained unresolved. On the contrary, the ^{113}Cd NMR spectrum of the well-studied rabbit liver $^{113}Cd_7$-MT-2a, remeasured in these studies, showed seven rather sharp and intense resonances between 610 and 680 ppm at 298 K (Table 2) (*32*, *33*). The signals possessed an apparent line width between 75 and 180 Hz

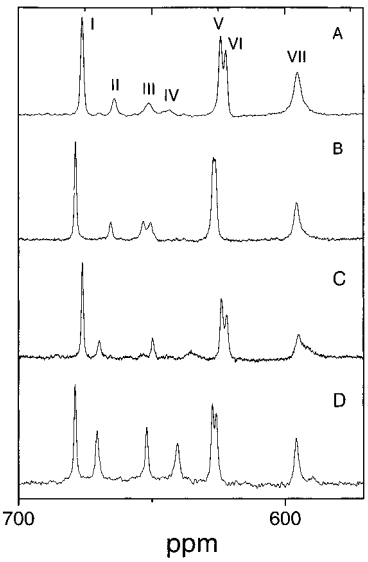

FIGURE 3: 133 MHz ^{113}Cd NMR spectra of human $^{113}Cd_7$-MT-3 at 298 K (A) and 323 K (B) (*16*) and of $^{113}Cd_7$-mutMT-3 at 298 K (C) and 323 K (D). Conditions: 2 mM protein sample in 25 mM Tris-HCl and 50 mM NaCl at pH 8.0.

Table 2: ^{113}Cd NMR Chemical Shift Position and Relative Intensity of ^{113}Cd Signals in $^{113}Cd_7$-MT-3 and $^{113}Cd_7$-mutMT-3 at 298 and 323 K[a]

	signal position [relative intensity (%)][b]				
	rabbit MT-2a	MT-3		mutMT-3	
	298 K	298 K	323 K	298 K	323 K
α-domain					
I	677	676	678	676	678
V	637	624	627	624	626
VI	631	622	626	622	626
VII	618	595	596	595	595
β-domain					
II	674	664 (20)	665 (20)	670 (25)	670 (65)
III	664	651 (25)	653 (30)	650 (20)	651 (80)
IV	655	644 (10)	650 (20)	635 (15)	639 (75)

[a] Since the intensity of the ^{113}Cd signals originating from the α-domain was comparable, only the intensities of signals of the β-domain are presented. For comparison, the chemical shift position of ^{113}Cd signals in $^{113}Cd_7$-MT-2a at 298 K, remeasured in this study, is also given. [b] The integral of the signal at lowest field (around 676 ppm) of each spectrum was set to 100%. Although no T_1 values for the ^{113}Cd resonances were determined, signal saturation could be ruled out, as identical signal intensities were obtained using 0.4 and 2 s pulse repetition rates.

and showed well-resolved homonuclear [^{113}Cd−^{113}Cd] couplings, features which previously enabled the determination of the cluster topology of $^{113}Cd_7$-MT-2a by [^{113}Cd, ^{113}Cd] COSY (see Table 2) (*32*, *33*). The chemical shift positions of the signals of $^{113}Cd_7$-MT-3 and $^{113}Cd_7$-mutMT-3 resemble those in $^{113}Cd_7$-MT-2a (Table 2), the only exception being the about 20 ppm high-field shift of signal VII compared to the range of the so far reported ^{113}Cd resonances of mammalian Cd_7-MTs. The increased shielding of this resonance may suggest an altered coordination environment of this metal-binding site.

The NMR features of $^{113}Cd_7$-mutMT-3 and $^{113}Cd_7$-MT-3 discussed above made a direct NMR determination of the cluster topology impossible. However, in $^{113}Cd_7$-MT-3 signals I and V−VII (Figure 3A,B) could be assigned to a $^{113}Cd_4CysS_{11}$ cluster in the α-domain of MT-3, based on the comparison with the ^{113}Cd NMR spectrum of the isolated $^{113}Cd_4$-α-domain of MT-3. Consequently, the remaining three minor signals of $^{113}Cd_7$-MT-3 (signals II−IV in Figure 3A) have been interpreted to originate from a Cd_3S_9 cluster in the β-domain (*16*). In $^{113}Cd_7$-mutMT-3 the four major signals are found at exactly the same chemical shift position as those of $^{113}Cd_7$-MT-3 (Table 2). This correspondence indicates that the Cd_4 cluster structure within the α-domain of both MT-3 forms possesses the same topology and that this structure is unaffected by the mutation of two proline residues in the β-domain. In contrast, the β-domain resonances occur at different chemical shift positions, due to the replacement of the two prolines in mutMT-3. The above results suggest that the partitioning of the seven Cd(II) ions in MT-3 and mutMT-3 into three- and four-metal clusters located in two protein domains is similar to that found in mammalian Cd_7-MTs.

Apart from broad and unresolved signals detected in both $^{113}Cd_7$-mutMT-3 and $^{113}Cd_7$-MT-3 at 298 K, another striking feature is the very low intensity (∼20%) of the β-domain resonances when compared to those of the α-domain (Figure 3A,C, Table 2). It should be noted that neither additional resonances were detected outside of the chemical shift range presented nor signal saturation of the β-domain resonances due to long T_1 relaxation times occurred. The latter could be ruled out since spectra recorded with a 0.4 and 2 s delay time showed the same pattern of signal intensity distribution. In addition, metal loss as the cause for this effect could also be excluded (see Materials and Methods). Thus, the presence of dynamic processes has to be responsible for these NMR features. This fact has been clearly documented in our detailed ^{113}Cd NMR studies of $^{113}Cd_7$-MT-3 (*16*).

However, a striking temperature effect on the β-domain resonances in $^{113}Cd_7$-mutMT-3 occurred compared to $^{113}Cd_7$-MT-3. Thus, while the signals of $^{113}Cd_7$-MT-3 remained unaffected upon the temperature rise from 298 to 323 K (*16*), those of $^{113}Cd_7$-mutMT-3 increased in intensity approximately from 20% to 70%. In both instances the signal intensity was compared to that of the α-domain resonances (Figure 3, Table 2). The reversibility of this process could be demonstrated by remeasuring the $^{113}Cd_7$-mutMT-3 at 298 K after keeping the sample for 20 h at 323 K. The temperature-treated sample exhibited at 298 K essentially the same ^{113}Cd NMR spectrum and intensity distribution as the freshly prepared $^{113}Cd_7$-mutMT-3 sample. These results clearly demonstrate that the two conserved proline residues in the β-domain of MT-3 have a profound effect on the dynamics of the three-metal cluster (see below).

Determination of Apparent Binding Constants for Cd(II)- and Zn(II)-Metalloforms. (A) Cd(II)-Binding Constants Determined through pH Titration. In this spectrophotometrical method, the determination of the apparent binding constants is based on the competition between protons and metals for cysteine thiolates (*23*, *25*). The decreasing intensities of the CysS−Cd(II) LMCT band at 250 nm of Cd_7-MT-3, Cd_7-mutMT-3, and Cd_7-MT-2a with progressive acidification are depicted in Figure 4. Rabbit Cd_7-MT-2a shows the previously established two-step titration profile, due to different metal-binding affinities of the two protein domains (*23*). However, in both Cd_7-MT-3 and Cd_7-mutMT-3 the pH separation between both domains is much less pronounced. In similar

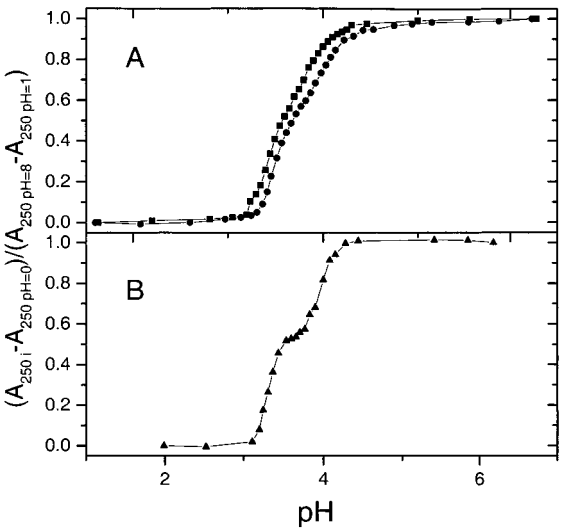

FIGURE 4: pH titration curves of (A) Cd_7-MT-3 (■) and Cd_7-mutMT-3 (●) and (B) rabbit liver Cd_7-MT-2 (△). For details, see Materials and Methods.

Table 3: Apparent Binding Constants of Human MT-3, mutMT-3 and Rabbit Liver MT-2a with Zn(II) and Cd(II) Ions

	K_{Cd}[a] (M^{-1})	K_{Zn}[b] (M^{-1})
MT-2	7.0×10^{14}	3.1×10^{11}
mutMT-3	3.7×10^{14}	2.4×10^{11}
MT-3	2.0×10^{14}	6.2×10^{10}

[a] Cd-binding constants were determined by the competition between metal ions and protons for the thiolate ligands and extrapolated to pH 7.0. For details, see Materials and Methods. [b] Zn-binding constants were determined by the competition between the protein and 5F-BAPTA at pH 8.0. For details, see Materials and Methods.

studies of Cd(II)-containing MT from various species, the presence of a more or less pronounced two-step titration profile has also been observed (*22*, *23*). The average apparent binding constants of Cd_7-MT-3, Cd_7-mutMT-3, and Cd_7-MT-2a lie in the same range (Table 3). The determined binding constant for rabbit liver Cd_7-MT of 7×10^{14} M^{-1} is similar to those previously reported for a number of other Cd_7-MTs from various species using the same method, i.e., 1.25×10^{15} M^{-1} for rabbit liver Cd_7-MT (*23*), or by voltametric measurements, i.e., $(6-10) \times 10^{14}$ M^{-1}, pH 7.5, for rabbit liver Cd_7-MT (*34*).

(B) Zn(II)-Binding Constants Determined by ^{19}F NMR of 5F-BAPTA. The fluorinated complexing agent 5F-BAPTA was originally used to determine free metal concentrations in biological fluids by ^{19}F NMR (*35*, *36*). Since the chemical shift positions of the ^{19}F signal for free 5F-BAPTA and its complexes with various metal ions differ, it is possible to measure the free concentration of two metals such as Zn(II) and Ca(II) simultaneously (*25*, *37*). As 5F-BAPTA forms a 1:1 complex with divalent metal ions, the integrals of the ^{19}F signals are directly proportional to the concentrations of metal-bound and free 5F-BAPTA, respectively.

The ^{19}F NMR spectra of a mixture of 5F-BAPTA with either Zn_7-mutMT-3, Zn_7-MT-3, or rabbit liver Zn_7-MT-2a showed in each case two signals at −116 and −121 ppm, which correspond to the Zn-5F-BAPTA complex and free 5F-BAPTA, respectively (data not shown). They reflect partitioning of zinc between the protein and the reagent. The apparent Zn-binding constants of the three proteins Zn_7-MT-3, Zn_7-mutMT-3, and Zn_7-MT-2a were obtained according to the expression given in the Appendix (for details, see Materials and Methods) and are summarized in Table 3. Similarly to the Cd(II) complexes, the apparent binding constants of all three Zn(II) proteins lie in the same range.

The value of 3.1×10^{11} M^{-1} obtained for rabbit liver Zn_7-MT-2a is comparable to those obtained for various mammalian Zn_7-MTs by other methods and under different conditions, demonstrating the feasibility of this method for the determination of metal-binding constants. Thus, voltametric measurements revealed binding constants for horse kidney Zn_7-MT of $(2.5-5.0) \times 10^{11}$ M^{-1} and for rabbit liver Zn_7-MT of $(8-12) \times 10^{11}$ M^{-1} (both at pH 7.5) (*34*). For equine liver Zn_7-MT a pH titration method revealed a constant of 2×10^{12} M^{-1} at pH 7.0 (*21*).

DISCUSSION

The biological studies on the MT-3 mutants clearly established the necessity of both proline residues for the inhibitory activity, as even single mutants were found to be inactive (see Figure 1). The results obtained with the double mutant Zn_7-mutMT-3 are similar to those obtained on the isolated Zn_3-β-domain, where the same mutation of the C(6)-P-C-P(9) motif to C(6)-S-C-A(9) abolishes the biological activity (*13*). However, both Zn_7-MT-3 and the isolated Zn_3-β-domain exhibit a similar degree of inhibitory activity, suggesting that the presence of the α-domain is without an effect. This observation raises the question regarding the biological role of this protein domain. With the aim to shed light into the underlying differences likely responsible for the biological activity, the double mutant mutMT-3 was further investigated regarding its structural and metal-binding properties and compared to wild-type human MT-3 and rabbit MT-2a.

In earlier biological studies on wild-type MT-3, specific structural properties of the protein or an altered zinc affinity for MT-3 compared to that for MTs have been considered as a possible reason for the observed biological activity (*38*, *39*). The latter may affect the intracellular zinc donation and/or redistribution. The determined apparent binding constants of MT-3, mutMT-3, and MT-2a with Zn(II) and Cd(II) ions, summarized in Table 3, exhibit the same trend for both metals; i.e., MT-2a shows the highest and MT-3 the lowest affinity and the binding constants of mutMT-3 are in between. However, the differences in the apparent binding constants are rather small, indicating that the metal−thiolate clusters of MT-3 are thermodynamically comparable to that of MT-2a. The decreased binding constants for both MT-3 and mutMT-3 are most likely due to an increased electrostatic repulsion between the substantially larger overall negative charge of the polypeptide chain (−3 vs +4 in apoMT-2a at pH 7.0) and the negatively charged metal−thiolate clusters (−3 each). In recent semiempirical calculations, it has been shown that within the β-domain of rat MT-2 all bridging Cys residues, especially Cys(7), are crucial for metal binding (*40*). The corresponding Cys(8) in MT-3 is flanked by the two Pro residues which may partially destabilize the metal−thiolate cluster compared to mutMT-3. Taking together the closely similar apparent binding constants for MT-2a, MT-3, and mutMT-3 suggests that differences in metal binding affinities do not play a crucial role in the biological activity of MT-3.

The CD spectra, which are sensitive to the cluster geometry, revealed marked differences in shape and band positions. Thus, while the two CD extrema of Cd_7-mutMT-3 and Cd_7-MT-2a at 238 and 261 nm, originating from CysS−Cd(II) LMCT bands, are found at the same wavelengths, the CD profile displayed by Cd_7-MT-3 is blue shifted (Figure 2). The latter features point to an altered structure of the Cd_3S_9 cluster in the β-domain of MT-3, which must be attributed to the presence of the two proline residues in this protein. This conclusion is supported by the fact that these changes are largely abolished in the double mutant Cd_7-mutMT-3. In the high-energy CD region (below 240 nm), there are additional differences discerned between the Cd_7-MT-3/Cd_7-mutMT-3 pair and Cd_7-MT-2. Thus, while the latter form exhibits a pronounced positive CD extremum around 228 nm, both CD profiles of the MT-3 pair show a negative trough. A possible explanation for the difference between these CD spectra in the high-energy region could be the presence of an α-helix in the tertiary structure of Cd_7-MT-3 and Cd_7-mutMT-3. A typical negative CD band of the protein α-helix is expected near 225 nm. The presence of such a feature in MT-3/mutMT-3 would result in a compensatory effect on the original positive CD profiles resulting in the observed negative CD features. Indeed, secondary structure predictions on the dodecapeptide loop connecting Cys(51)−Cys(64) in the primary structure of MT-3, which includes the conserved hexapeptide insert, show a high probability for an α-helical structure (90%) (*41*).

More detailed information regarding the structural influence of the two prolines can be drawn from the ^{113}Cd NMR studies. Whereas the four major ^{113}Cd resonances in both $^{113}Cd_7$-mutMT-3 and $^{113}Cd_7$-MT-3, originating from the Cd_4S_{11} cluster in the α-domain, occur at exactly the same chemical shift position, chemical shifts of the $^{113}Cd_3S_9$ cluster resonances in $^{113}Cd_7$-mutMT-3 differ (Figure 3A,C). This is not surprising in view of the sensitivity of ^{113}Cd NMR to minor alterations of the coordination geometry. However, both MT-3 forms exhibit striking differences upon the temperature rise. Thus, while $^{113}Cd_7$-MT-3 shows a very low and temperature-independent intensity of the ^{113}Cd resonances of the β-domain (∼20%), the corresponding resonances of $^{113}Cd_7$-mutMT-3 increase in intensity on going from 298 to 323 K from approximately 20% to 70%, respectively (Table 2). Thus the mutation of the two proline residues not only abolished the biological activity but also gave rise to a markedly different temperature behavior of the Cd_3S_9 cluster resonances.

In our previous ^{113}Cd NMR studies of $^{113}Cd_7$-MT-3, the significant broadening of all NMR signals and the very low and temperature-independent intensity of the Cd_3S_9 cluster resonances have been interpreted in terms of dynamic processes acting on two different NMR time scales: (i) fast exchange processes among *conformational* cluster substates brought about by minor dynamic alterations of the metal coordination geometry in both clusters and (ii) additional very slow exchange processes within the β-domain connected with the formation of *configurational* cluster substates (*16*). The latter can be visualized as major structural fluctuations due to temporarily breaking and re-forming of the metal−thiolate bonds (*42*). Since signals from the majority of configurational substates are exchange-broadened beyond detection limits, the observed signals of the β-domain would reflect only a minor part of the Cd_3S_9 cluster population (*16*). We suggest that similar dynamic processes occur also in $^{113}Cd_7$-mutMT-3. In this case, however, the mutation of both prolines recovered about 70% intensity of the Cd_3S_9 cluster resonances upon raising the temperature to 323 K. In this connection the question arose regarding the presence of similar cluster dynamics in well-studied mammalian MT-1/MT-2 isoforms. A closer inspection of the reported temperature behavior of rabbit liver Cd_7-MT-2a revealed that the ^{113}Cd resonances originating from the β-domain showed at 298 K about 70% intensity compared to those of the α-domain. However, upon temperature rise to 323 K the intensity of the β-domain resonances increased almost to that of the α-domain (*32*). Thus, it would appear that similar cluster dynamics also exist within the β-domain of this protein.

The different folding properties of the polypeptide chain in the β-domain of MT-3, owing to the presence of the proline residues, have to be responsible for the marked differences in its NMR behavior. Prolines are often found to be key amino acids in the secondary structure formation of proteins. The probability of finding a particular amide bond Xaa−Yaa in the *cis* instead of a *trans* conformation is in the case of all amino acids Yaa other than Pro in the range of 10^{-3} (*43*). In contrast, Xaa−Pro peptide bonds have a much higher probability of being in the *cis* conformation. From 617 nonredundant protein structures 43% contained at least one *cis* peptidyl−prolyl bond (*44*), or in a similar quantification 5.7% of the total Xaa−peptide bonds in globular proteins were found in the *cis* form (*45*). During the folding process some off-pathway folding events, requiring *cis/trans* interconversion of Xaa−Pro amide bonds, take much longer time and have therefore often been found to be the rate-limiting step (*44*). This is exemplified by relaxation times for the *cis/trans* isomerization of proline residues in proteins ranging between 10 and hundreds of seconds (*46*, *47*). Moreover, the ^{1}H NMR spectra of small, nonstructured peptides usually display a second set of amide resonances for residues close to prolines, indicating that *cis/trans* interconversion is slow on the ^{1}H NMR time scale (*47*).

The 3D structures of mammalian MT-1/MT-2 are characterized by the lack of longer stretches of well-defined secondary structure elements. In these proteins coordinative bonds between cysteine thiolates and metal ions define the direction of the polypeptide chain. Moreover, the buried metal−thiolate clusters show a marked kinetic lability characterized by easy metal exchange confined predominately to the less structurally constrained β-cluster, where a half-life of 0.5 s was found (*24*, *32*). In view of the high sequence identity between MT-3 and mammalian MT-1/MT-2 (approximately 70%), the overall fold of both proteins may be rather similar.

To account for our NMR results on the β-domain of MT-3 and mutMT-3, we propose that well-established structural processes in proteins involving a reversible partial structure unfolding occur. This dynamic feature may account for the established kinetic lability of the metal−thiolate clusters. In view of the high apparent metal-binding constants for MT-3 and mutMT-3 (see above) the metal ions in the partially unfolded state do not dissociate from the protein, and therefore, this state may somewhat resemble the molten globule state, i.e., a conformation which is neither fully

folded nor unfolded. Concomitantly with this process, solvent access and its binding would most probably occur. This would be characterized by a very rapid interconversion of coordination isomers leading to an extensive exchange broadening of the ^{113}Cd resonances making them nondetectable.

In the case of mutMT-3, a major part of the signal intensity of the β-domain resonances was recovered upon the temperature rise. Two effects might be responsible for this finding. First, the temperature rise could thermodynamically favor the closed detectable cluster population. Such a dramatic effect cannot be due only to a change in the Boltzman distribution with unchanged free energy of both states. We therefore infer that the free energy of the opened and/or closed states would have to change. Assuming that the fully folded state is thermodynamically more stable, the recovery of signal intensity with increasing temperature would imply an increased stability of the protein at higher temperature. Such a behavior is not unusual, since a so-called "cold denaturation" was observed with several proteins (*48*). Second, a kinetic effect could lead to a faster exchange between the detectable and nondetectable populations, making parts of the undetectable population accessible to NMR detection.

In contrast to mutMT-3, no recovery of signal intensity of the β-domain resonances with increasing temperature was observed in wild-type MT-3. We suggest that during the transition from the partially unfolded to the folded state an additional process occurs, involving *cis/trans* isomerization of Cys−Pro(7) or Cys−Pro(9) amide bonds. The slow *cis/trans* interconversion, required for correct protein refolding, would then become a rate-limiting step. Apparently, the temperature rise to 323 K would be not sufficient to overcome the activation barrier for this process. This conclusion is supported by thermodynamic parameters for the Xaa−Pro *cis/trans* isomerization. The activation energy ΔE_a of 55 kJ mol^{-1} is rather high compared to the difference in free energy between a *cis* and a *trans* proline ($\Delta G°$ *cis/trans* ∼4−8 kJ mol^{-1}) (*49*). Consequently, a significant population of the partially unfolded β-domain would be kinetically trapped in the state in which the metal−thiolate cluster is nondetectable (see above). In the recent Zn *K*-edge EXAFS studies of Zn_7-MT-3 and its Zn_3-β-domain at 77 K, a very short Zn−Zn distance of 3.2 Å was found (*50*). Such a short distance is incompatible with the crystallographically determined cyclohexane-like cluster structure in the β-domain of rat MT-2, in which a much larger distance exists (3.8 Å) (*51*). It is conceivable that the short Zn−Zn distance in Zn_7-MT-3 might represent the NMR nondetectable population(s) of the $M^{II}_3S_9$ cluster structure. Overall, from the comparison of the NMR behavior of wild-type MT-3 and mutMT-3, it can be concluded that a partial unfolding of the β-domain is an important structural event and that the kinetics of this process is mainly determined by the *cis*/*trans* interconversion of Cys−Pro amide bonds.

In summary, the biological and structural studies presented on MT-3 and MT-3 mutants indicate that specific structural features dictated by the repetitive $(Cys\text{-}Pro)_2$ sequence in the β-domain of MT-3 and not its altered metal-binding affinity compared to MT-1/MT-2 are responsible for its biological activity. It has been shown that repetitive $(Xaa\text{-}Pro)_n$ sequences in proteins can function as stiff "sticky arms", allowing the rapid and reversible binding to other proteins (*14*). At present, it is not known whether the fully folded or partially unfolded state is important for biological activity of MT-3. However, as sampling of conformational space is important for protein−protein interaction, the more flexible open state would be favored in this process. In contrast to Pro-rich regions in other proteins involved in protein−protein interactions, the C(6)-P-C-P(9) recognition sequence in MT-3 would be substantially stabilized by the binding of the flanking cysteines to metal ion(s). The latter feature would represent a novel biological role for the metal−thiolate clusters in MTs.

ACKNOWLEDGMENT

The authors thank Dr. I. Jelezarov for a helpful comment, N. Walch and M. Binder for recording the NMR spectra, and Dr. P. Gehrig for obtaining the ESI-MS spectra.

SUPPORTING INFORMATION AVAILABLE

An appendix containing the derivation of the equation used in the calculation of the apparent binding constants that were determined through the competition between the protein and 5F-BAPTA. This material is available free of charge via the Internet at http://pubs.acs.org.

REFERENCES

1. Selkoe, D. J. (1991) *Neuron 6*, 487−498.
2. Appel, S. H. (1981) *Ann. Neurol. 10*, 499−505.
3. Uchida, Y., Ihara, Y., and Tomonaga, M. (1988) *Biochem. Biophys. Res. Commun. 150*, 1263−1267.
4. Uchida, Y., Takio, K., Titani, K., Ihara, Y., and Tomonaga, M. (1991) *Neuron 7*, 337−347.
5. Palmiter, R. D., Findley, S. D., Whitmore, T. E., and Durnam, D. M. (1992) *Proc. Natl. Acad. Sci. U.S.A. 89*, 6333−6337.
6. Tsuji, S., Kobayashi, H., Uchida, Y., Ihara, Y., and Miyatake, T. (1992) *EMBO J. 11*, 4843−4850.
7. Pountney, D. L., Fundel, S. M., Faller, P., Birchler, N. E., Hunziker, P., and Vašák, M. (1994) *FEBS Lett. 345*, 193−197.
8. Kobayashi, H., Uchida, Y., Ihara, Y., Nakajima, K., Kohsaka, S., Miyatake, T., and Tsuji, S. (1993) *Brain Res. Mol. Brain Res. 19*, 188−194.
9. Chen, C. F., Wang, S. H., and Lin, L. Y. (1996) *Comp. Biochem. Physiol., Part B: Biochem. Mol. Biol. 115*, 27−32.
10. Kojima, S., Shimada, A., Kodan, A., Kobayashi, K., Morita, T., Yamano, Y., and Umemura, T. (1998) *Can. J. Vet. Res. 62*, 148−151.
11. Erickson, J. C., Sewell, A. K., Jensen, L. T., Winge, D. R., and Palmiter, R. D. (1994) *Brain Res. 649*, 297−304.
12. Bruinink, A., Faller, P., Sidler, C., Bogumil, R., and Vašák, M. (1998) *Chem.-Biol. Interact. 115*, 167−174.
13. Sewell, A. K., Jensen, L. T., Erickson, J. C., Palmiter, R. D., and Winge, D. R. (1995) *Biochemistry 34*, 4740−4747.
14. Williamson, M. P. (1994) *Biochem. J. 297*, 249−260.
15. Faller, P., and Vašák, M. (1997) *Biochemistry 36*, 13341−13348.
16. Faller, P., Hasler, D. W., Zerbe, O., Klauser, S., Winge, D. R., and Vašák, M. (1999) *Biochemistry 38*, 10158−10167.
17. Arseniev, A., Schultze, P., Wörgötter, E., Braun, W., Wagner, G., Vašák, M., Kägi, J. H. R., and Wüthrich, K. (1988) *J. Mol. Biol. 201*, 637−657.
18. Vašák, M. (1991) *Methods Enzymol. 205*, 41−44.
19. Vašák, M. (1991) *Methods Enzymol. 205*, 452−458.
20. Pedersen, A. O., and Jacobsen, J. (1980) *Eur. J. Biochem. 106*, 291−295.
21. Vašák, M., and Kägi, J. H. R. (1983) in *Metal ions in biological systems* (Sigel, H., Ed.) pp 213−273, Marcel Dekker Inc., New York and Basel.

22. Kägi, J. H. R., and Vallee, B. (1961) *J. Biol. Chem. 236*, 2435−2442.
23. Wang, Y., Mackay, E. A., Kurasaki, M., and Kägi, J. H. (1994) *Eur. J. Biochem. 225*, 449−457.
24. Vašák, M., and Kägi, J. H. R. (1994) in *Encyclopedia of Inorganic Chemistry* (King, R. B., Ed.) pp 2229−2241, J. Wiley & Sons Ltd., New York.
25. Long, G. J., Rosen, J. F., and Schanne, F. A. (1994) *J. Biol. Chem. 269*, 834−837.
26. Schoenmakers, T. J., Visser, G. J., Flik, G., and Theuvenet, A. P. (1992) *BioTechniques 12*, 870−874.
27. Vašák, M., Kägi, J. H. R., and Hill, H. A. (1981) *Biochemistry 20*, 2852−2856.
28. Willner, H., Vašák, M., and Kägi, J. H. (1987) *Biochemistry 26*, 6287−6292.
29. Henehan, C. J., Pountney, D. L., Zerbe, O., and Vašák, M. (1993) *Protein Sci. 2*, 1756−1764.
30. Stillman, M. J. (1992) in *Metallothioneins* (Stillman, M. J., Shaw, C. F. I., and Suzuki, K. T., Eds.) pp 55−127, VCH, New York.
31. Willner, H., Bernhard, W. R., and Kägi, J. H. R. (1992) in *Metallothioneins* (Stillman, M. J., Shaw, C. F. I., and Suzuki, K. T., Eds.) pp 128−143, VCH, New York.
32. Nettesheim, D. G., Engeseth, H. R., and Otvos, J. D. (1985) *Biochemistry 24*, 6744−6751.
33. Frey, M. H., Wagner, G., Vašák, M., Sorensen, O. W., Neuhaus, D., Wörgötter, E., Kägi, J. H. R., Ernst, R. R., and Wüthrich, K. (1985) *J. Am. Chem. Soc. 107*, 6847−6851.
34. Munoz, A., and Rodriguez, A. R. (1995) *Electroanalysis 7*, 674−680.
35. Smith, G. A., Hesketh, R. T., Metcalfe, J. C., Feeney, J., and Morris, P. G. (1983) *Proc. Natl. Acad. Sci. U.S.A. 80*, 7178−7182.
36. Levy, L. A., Murphy, E., and London, R. E. (1987) *Am. J. Physiol. 252*, C441−449.
37. Benters, J., Flogel, U., Schafer, T., Leibfritz, D., Hechtenberg, S., and Beyersmann, D. (1997) *Biochem. J. 322*, 793−799.
38. Erickson, J. C., Hollopeter, G., Thomas, S. A., Froelick, G. J., and Palmiter, R. D. (1997) *J. Neurosci. 17*, 1271−1281.
39. Palmiter, R. D. (1995) *Toxicol. Appl. Pharmacol. 135*, 139−146.
40. Chang, C. C., Liao, W. F., and Huang, P. C. (1998) *Protein Eng. 11*, 41−46.
41. Hasler, D. W., Faller, P., and Vašák, M. (1998) *Biochemistry 37*, 14966−14973.
42. Hagen, K. S., Stephan, D. W., and Holm, R. H. (1982) *Inorg. Chem. 21*, 3928−3936.
43. Ramachandran, G. N., and Mitra, A. K. (1976) *J. Mol. Biol. 107*, 85−92.
44. Schmid, F. X. (1993) *Annu. Rev. Biophys. Biomol. Struct. 22*, 123−142.
45. MacArthur, M. W., and Thornton, J. M. (1991) *J. Mol. Biol. 218*, 397−412.
46. Reimer, U., Scherer, G., Drewello, M., Kruber, S., Schutkowski, M., and Fischer, G. (1998) *J. Mol. Biol. 279*, 449−460.
47. Grathwohl, C., and Wüthrich, K. (1981) *Biopolymers 20*, 2623−2633.
48. Privalov, P. L. (1990) *Crit. Rev. Biochem. Mol. Biol. 25*, 281−305.
49. Wüthrich, K., and Grathwohl, C. (1974) *FEBS Lett. 43*, 337−340.
50. Bogumil, R., Faller, P., Binz, P. A., Vašák, M., Charnock, J. M., and Garner, C. D. (1998) *Eur. J. Biochem. 255*, 172−177.
51. Robbins, A. H., McRee, D. E., Williamson, M., Collett, S. A., Xuong, N. H., Furey, W. F., Wang, B. C., and Stout, C. D. (1991) *J. Mol. Biol. 221*, 1269−1293.

BI001569F